Fundamentals of chaos

Warwick Tucker

University of Bergen
Department of mathematics
5008, Bergen, Norway
warwick.tucker@math.uib.no

1 Introduction

In this chapter, we will give a brief introduction to some aspects of chaos theory. This task is by no means easy: despite more than four decades of intense research in this area, there is still no general agreement as to what the word *chaos* should really mean. In fact, there appears to exist almost a continuum of definitions of a *chaotic* system, all slightly tweaked to suit each researcher's specific needs. In this overview, we will present several chaotic systems, such as discrete interval maps and three-dimensional continuous strange attractors.

This account does by no means give a complete introduction to the vast theory of chaotic dynamical systems. For some nice, and more comprehensive, introductions to this topic, we refer to e.g. [HW91, Ro95, PT93, Vi97].

2 Dynamical Systems

A *dynamical system* is a set of rules that maps a state into the future. A simple example is a function f acting on some *state space* U, sometimes also referred to as the *phase space*. Given $f\colon U \to U$, we can consider consecutive *iterates* of an initial point $x_0 \in U$:

$$x_{n+1} = f(x_n), \qquad n \in \mathbb{N}. \tag{1}$$

It is customary to use the notation $f^0(x_0) = x_0; f^{n+1}(x_0) = f(f^n(x_0))$. The sequence of iterates $\{f^i(x)\}_{i=0}^{\infty}$ is called the *forward orbit* of x under f. If the map f is invertible, we can also talk about the *backward orbit* $\{f^{-i}(x)\}_{i=0}^{\infty}$. In this setting, we think of the time as being discrete, and labelled by the index i. Pairing the time variable with the space variable gives the following view of the evolution of the dynamical system:

$$(t_0, x_0), (t_1, f(x_0)), \ldots, (t_n, f^n(x_0)), \ldots \tag{2}$$

The main questions we are interested in relate to the long-term behavior of the dynamical system: what is the asymptotic behavior of the orbits? Does this depend on the choice of the initial condition x_0? And how does it depend on small variations of f? These are all questions that are instrumental in the theory of dynamical systems.

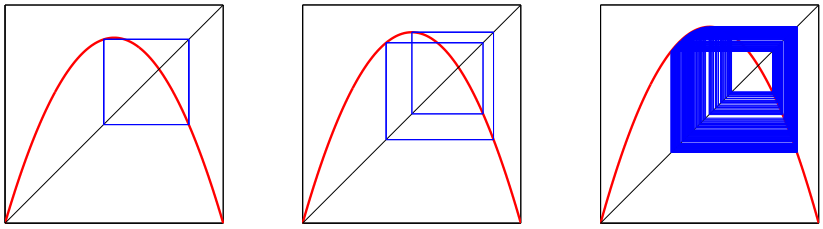

Fig. 1. Iterates 100 to 1000 of f_a with (a) $a = 3.4$ (b) $a = 3.5$ (c) $a = 3.6$.

Example 1. As a simple illustration, we consider the one-parameter function $f_a\colon [0,1] \to [0,1]$, defined by $f_a(x) = ax(1-x)$, where $a \in [0,4]$. For the parameter values $a = 3.4$ and $a = 3.5$, the iterates of $x_0 = 0.25$ converge to a periodic orbit, see Fig. 1(a,b). In fact, almost any choice of $x_0 \in I$ will display the same asymptotics. That the limiting behavior of the dynamical system is very regular is also apparent from the histogram of the iterates, see Fig. 2(a,b).

If we change the parameter to $a = 3.6$, the situation changes dramatically. No longer is the trajectory confined to small regions of the phase space, see Fig. 1(c). As the histogram in Fig. 2(c) indicates, the orbit repeatedly visits almost every portion of the union of two intervals.

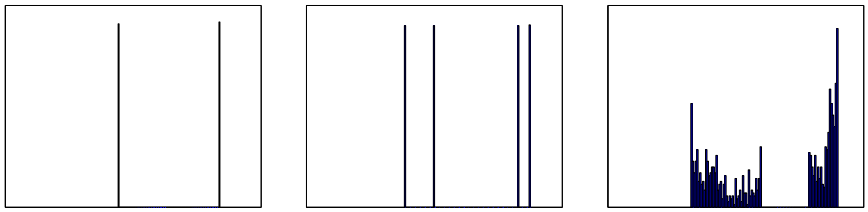

Fig. 2. Histograms of the 4000 first iterates of f_a with (a) $a = 3.4$ (b) $a = 3.5$ (c) $a = 3.6$.

The fundamentally different behaviors of the system of Example 1 indicates that the system undergoes some *bifurcations* as the parameter a is varied. We will return to this topic later.

Another important class of dynamical systems are given by differential equations $\dot{x} = f(x)$. Now, the time is thought of as being continuous. Let us denote the solution (or *flow*) by $\varphi(x,t)$, i.e., we have

$$\frac{d}{dt}\varphi(x,t) = f(\varphi(x,t)), \qquad \varphi(x,0) = x. \tag{3}$$

We can then ask exactly the same questions about the long-term behavior of this dynamical system as above.

Example 2. Let us consider the following one-parameter planar polynomial vector field:

$$\begin{aligned} \dot{x} &= x^2 + y^2 + a \\ \dot{y} &= y^2 - x^4. \end{aligned}$$

Plotting the solutions to the system with $a = 2$ reveals no interesting dynamics, see Fig. 3(a). In the natural (x,y)-coordinate frame, all solutions flow from $y = +\infty$ to $y = -\infty$. Thus the dynamics is entirely made up of transients. Setting $a = -2$, however, produces a system with several fixed points of varying character, see Fig. 3(b). As a consequence, the solutions display a more rich behavior, including *sensitive dependence of initial conditions* – which we will return to later.

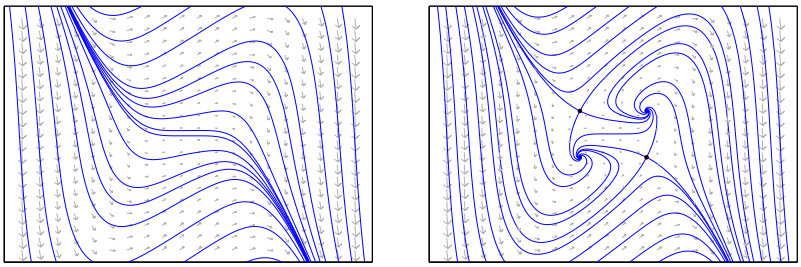

Fig. 3. (a) Regular flow with no fixed points for $a = 2$. (b) Two saddles, one spiral source, and one spiral sink for $a = -2$.

3 Fixed points

Given a dynamical system in terms of an iterated map (1), the simplest orbit is that of a *fixed point*, i.e., a point x^* that remains unaltered by the map

itself: $x^* = f(x^*)$. For a differential equation (3), a fixed point x^* corresponds to a vanishing vector field: $f(x^*) = 0$. In what follows, we will let $\mathrm{Fix}(f)$ denote the fixed points of f.

Assuming that f is at least C^1, it is the linearization $Df(x^*)$ of the system that, generically, reveals the character of the fixed point. We say that a fixed point is *hyperbolic* if there is expansion/contraction in all eigenspaces of the linearized system. For maps[1], this means that no eigenvalues of the matrix $Df(x^*)$ lie on the unit circle. Eigenspaces in which we have contraction are called *stable*; those in which we have expansion are called *unstable*.

A fixed point of a map whose linearization has only real eigenvalues of modulus less (greater) than one is called a *sink* (*source*). If it has eigenvalues of both types, it is called a *saddle*. In dimensions greater than one, the eigenvalues can be complex-valued; they then come in conjugate pairs. In the planar case, a fixed point having a pair of non-real eigenvalues inside (outside) the unit disc is called a *spiral sink* (*spiral source*), see Fig. 4. Of course, in higher dimensions, we can have combinations of the above. The point is that, at a hyperbolic fixed point, we can give an approximate description of the local behavior of the dynamical system. This is made more precise by the Hartman-Grobman Theorem:

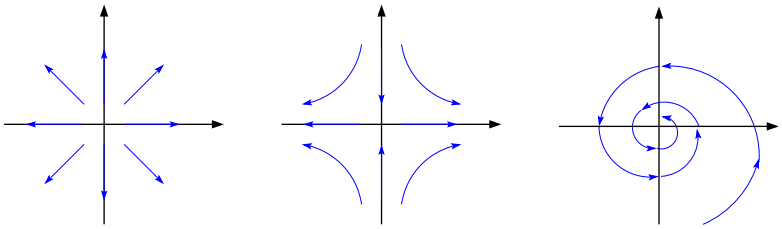

Fig. 4. Phase portraits of (a) a source, (b) a saddle, (c) a spiral sink.

Theorem 1 (Hartman-Grobman). *Let $U \subset \mathbb{R}^n$ be open, and let $f \in C^1(U, \mathbb{R}^n)$. If $x^* \in U$ is a hyperbolic fixed point of f, then there exists a homeomorphism h that maps a neighborhood of x^* to a neighborhood of the origin, and such that $h \circ f = Df(x^*) \circ h$.*

For differential equations the Hartman-Grobman theorem says that the flows $\varphi(x,t)$ and $\varphi_{x^*}(x,t)$ of the original, and linearized vector fields, respectively, can be conjugated near a fixed point x^*:

$$h(\varphi(x,t)) = \varphi_{x^*}(h(x),t). \tag{4}$$

[1] For differential equations the imaginary axis plays the same role as the unit circle does for maps. Eigenvalues with negative real parts correspond to stable eigenspaces.

For a proof of this theorem, and some differentiable variants, see [Be78, Ha60, Ha64, Ne64, Se85, St57, St58]. In principle, this theorem tells us that the dynamics near a hyperbolic fixed point is close to that of the linearized system, in the topological sense. From a qualitative point of view, this is very useful, seeing that we can completely analyze the linear system. From a quantitative point of view, however, we are not given much information about the homeomorphism h. In particular, we have no idea how large the neighborhood U can be taken. In order to obtain estimates of this type, a very careful analysis must be carried out. In the case of a saddle fixed point, the relative sizes of the eigenvalues may play a delicate role, see e.g. [Si52].

We emphasize the importance of demanding that the fixed point be hyperbolic. If this were not the case, an arbitrarily small perturbation could alter the dynamics completely. Thus hyperbolicity guarantees (local) robustness for the system.

Example 3. Returning to the quadratic map $f_a(x) = ax(1-x)$ of Example 1, we see that it has at most two fixed points: one at the origin, and (for $a > 1$) one at $x_a^* = 1 - \frac{1}{a}$. The linearizations at these fixed points are $Df(0) = a$, and $Df(x^*) = a(1-2x^*) = a-2$, respectively. This implies that the origin is stable for $a \in [0,1)$, and unstable for $a > 1$. The second fixed point is stable for $a \in (1,3)$, and unstable for $a > 3$.

Example 4. Returning to the vector field of Example 2, we see that its first component $\dot{x} = x^2+y^2+a = 0$ has no real solutions for $a = 2$. Thus the system lacks fixed points for this parameter value. For $a = -2$, however, the first component has an entire continuum of solutions: $x^2+y^2 = 2$. Propagating this constraint into the second component $\dot{y} = y^2 - x^4 = 0$, yields four solutions: $(1,1), (1,-1), (-1,1), (-1,-1)$. The linearization of the vector field is given by the Jacobian matrix:

$$Df(x,y) = \begin{pmatrix} 2x & 2y \\ -4x^3 & 2y \end{pmatrix}. \tag{5}$$

Inserting the coordinates for the fixed points into (5), and computing the eigenvalues of the resulting matrices is straight-forward. It reveals that the fixed points are of type: spiral source, saddle, saddle, and spiral sink, respectively.

4 Periodic orbits

Following the fixed point, the simplest dynamical object is a *periodic orbit*. For a map f, a point x_0 is said to have period $n \geq 1$ if $f^n(x_0) = x_0$. It has *principal* period n if n is minimal. The corresponding periodic orbit is the (finite) set of points $\{x_0, x_1, \ldots, x_{n-1}\}$. Note that this set is invariant under

the map f. In what follows, we let $\mathrm{Per}_n(f)$ denote the set of principal period-n orbits of f.

Just like with fixed points, we can study the stability of periodic orbits. These objects can be attracting, repelling, of saddle type, etc. For a map f, we simply note that a period-n point x_0 is a fixed point of the map $g = f^n$. Thus we can apply all theory about fixed points to g, and this directly carries over to the period-n orbit of f. In practice, it is useful to note that we have the following identity:

$$Dg(x_0) = D(f^n)(x_0) = \prod_{i=0}^{n-1} Df(x_i), \tag{6}$$

which is a direct consequence of the chain rule:

$$\begin{aligned} D(f^n)(x_0) = D(f(f^{n-1}))(x_0) &= Df(f^{n-1}(x_0))D(f^{n-1})(x_0) \\ &= Df(x_{n-1})D(f^{n-1})(x_0). \end{aligned}$$

In other words, the Jacobian matrix of $g = f^n$, evaluated at x_0, is the product of the n Jacobians of the map f, evaluated along the periodic orbit.

Consider the following ordering of the positive integers:

$$\begin{aligned} &3 > 5 > 7 > 9 > \cdots > 2\cdot 3 > 2\cdot 5 > 2\cdot 7 > \cdots > \\ &\quad 2^2\cdot 3 > 2^2\cdot 5 > 2^2\cdot 7 > \cdots > 2^3 > 2^2 > 2 > 1. \end{aligned}$$

A well-known result for maps is the following:

Theorem 2 (Sharkovsky). *Let $f\colon M \to M$ be a continuous map, where M is an interval or the real line. If f has a periodic point of period m and $m > n$ in the above ordering, then f also has a periodic point of period n.*

In particular, this means that if f has a period-3 orbit, then it has orbits of all periods. Note that this theorem is topological, and thus reveals nothing about the stability of the periodic orbits.

4.1 Flows and their return maps

We will now describe a useful relation between discrete-time (maps) and continuous-time (flows) dynamical systems. Consider the system of ordinary differential equations

$$\dot{x} = f(x), \tag{7}$$

where the vector field f is a C^k function: $f\colon \mathbb{R}^d \to \mathbb{R}^d$. Let $\varphi(x,t)$ denote the flow of (7), i.e.,

$$\tfrac{d}{dt}\varphi(x,t) = f(\varphi(x,t)),$$

and suppose that the system (7) has a periodic solution of period $\tau_0 > 0$, containing the point x_0, i.e., $\varphi(x_0, \tau_0 + t) = \varphi(x_0, t)$ for all $t \in \mathbb{R}$. Let Σ be

an $(d-1)$-dimensional surface transverse to the vector field at x_0, see Fig. 5. By this, we mean that the basis of Σ and the vector $f(x_0)$ span R^d, i.e., the flow is not tangent to Σ near x_0. Then we can find an open set $U \subset \Sigma$ containing x_0 such that for all $x \in U$, there exists a $\tau(x)$ close to τ_0 such that $\varphi(x, \tau(x)) \in \Sigma$. The point $\varphi(x, \tau(x))$ is called the *first return* of x, and

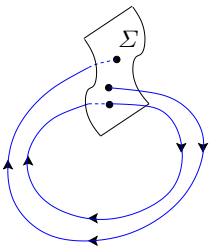

Fig. 5. The surface Σ and two trajectories.

the map R which associates a point with its first return is called the *return map*: $R(x) = \varphi(x, \tau(x))$. Note that, by construction, we have $\tau(x_0) = \tau_0$ and $R(x_0) = x_0$. Thus a fixed point of R corresponds to a periodic orbit of (7), and a periodic point of period n corresponds to a periodic orbit of (7) piercing Σ n times before closing.

One can show that, under the conditions stated above, and for sufficiently small U, the return map is a C^k diffeomorphism of U onto a subset of Σ. In other words: the return map is as smooth as the vector field. This means that, if $k \geq 1$, then the partial derivatives of R are well defined. By studying the Jacobian $DR(x_0)$ of the return map, we can determine the stability of the periodic orbit, as outlined in the previous section. We say that a periodic orbit γ of (7) is hyperbolic if any member of $\Sigma \cap \gamma$ is a hyperbolic periodic point for the return map R. In practice, we compute the Jacobian by solving the first variational equations associated to the flow. This is a d^2-dimensional linear system of differential equations which is solved along with the original d-dimensional system:

$$\dot{x}(t) = f(x(t)), \qquad x(0) = x_0, \tag{8}$$

$$\dot{v}(t) = Df(x(t))v(t), \qquad v(0) = I. \tag{9}$$

Whereas locating fixed points for a differential equation is a purely algebraic task (we simply solve the, possibly nonlinear, equation $f(x) = 0$), the task of finding periodic orbits is highly non-trivial. Indeed, it is not even known how many isolated periodic orbits a *planar, quadratic* differential equation can have. To this day, the record is 4, but nobody has yet proved that this is the true upper bound. This question is a part of Hilbert's 16th problem, which asks for the maximal number (and relative location) of limit cycles for planar polynomial differential equations. Even finding non-trivial *lower bounds* for

restricted families of planar polynomial vector fields poses a big challenge. For a recent overview of this problem, see [Il02].

5 Bifurcations

The theory of bifurcations deals with the behavior of a *family* of dynamical systems. In general, the family under study has finitely many parameters that change the character of the system's dynamics when varied. It is often the case that only one parameter is varied at a time; although in some situations two or maybe three parameters can be handled simultaneously.

Example 5. Consider the family of maps $E_a(x) = e^x - a$. We will study what happens to the dynamics as the scalar parameter a is varied.

For $a < 1$ the system has no fixed points. For $a = 1$ the origin is the unique fixed point (it solves the equation $e^x - 1 = x$). This fixed point is not hyperbolic: its associated eigenvalue is 1. When $a > 1$, there are two distinct hyperbolic fixed points, which have bifurcated from from the origin. One of these fixed points is stable; the other is unstable.

The transition as the parameter a passes through 1 is known as a *saddle-node-* or simply a *tangential* bifurcation. We illustrate the mechanism behind such a bifurcation in Fig. 6. The formal definition of a saddle-node bifurcation

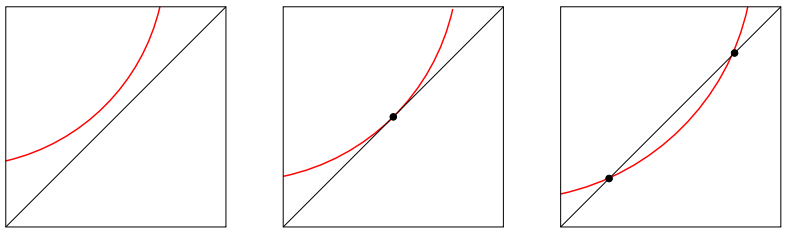

Fig. 6. The saddle-node bifurcation: (a) before, (b) during, and (c) after the bifurcation.

is stated below.

Definition 1 (saddle-node bifurcation). *A smooth, one-parameter family of maps $\{f_a\}$ undergoes a saddle-node bifurcation at a_0 if there exists an open interval I and a positive number ϵ such that*

(1) $a \in (a_0 - \epsilon, a_0) \Rightarrow \mathrm{Fix}(f_a|_I) = \emptyset$;
(2) $a = a_0 \Rightarrow \mathrm{Fix}(f_a|_I) = \{x^*\}$ *and* $f'_{a_0}(x^*) = 1$;
(3) $a \in (a_0, a_0 + \epsilon) \Rightarrow \mathrm{Fix}(f_a|_I) = \{x_1^*, x_2^*\}$.

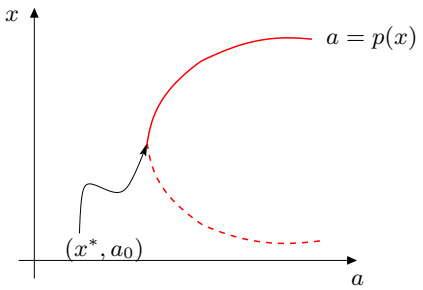

Fig. 7. The saddle-node bifurcation: the graph represents the location of the fixed points. It is dotted when unstable.

Of course, we may reverse the direction of the bifurcation with respect to the parameter a.

In the following theorem, explicit conditions are stated that imply the existence of a saddle-node bifurcation. Given a family of maps, the four conditions are easy to check. The proof relies on the implicit function theorem.

Theorem 3 (Saddle-node bifurcation). *Given a C^2 map f, assume that (1) $f_{a_0}(x^*) = x^*$, (2) $f'_{a_0}(x^*) = 1$, (3) $f''_{a_0}(x^*) \neq 0$, and (4) $\frac{\partial f_a}{\partial a}|_{a=a_0}(x^*) \neq 0$ hold. Then there exists an interval I containing the fixed point x^* and a smooth function $p\colon I \to \mathbb{R}$ with $p(x^*) = a_0$ such that $f_{p(x)}(x) = x$, $p'(x^*) = 0$, and $p''(x^*) \neq 0$.*

The graph of p describes the location of the two fixed points with respect to the parameter a, see Fig. 7.

We now turn to a second kind of bifurcation that can occur.

Example 6. Returning to the logistic family $f_a(x) = ax(1-x)$, recall from Example 3 that, when $a > 1$, there are two fixed points: the origin (unstable) and $x^*_a = 1 - \frac{1}{a}$, which is stable for $1 < a < 3$. When a passes through 3 the fixed point looses its stability: $f'_3(x^*_3) = -1$. In the range $3 < a < 3.445$, both the origin and x^*_a are unstable, and a stable period-2 orbit has bifurcated from x^*_a.

This is known as a *period doubling-* or simply a *flip* bifurcation. We illustrate the mechanism behind such a bifurcation in Fig. 8.

We formalize the bifurcation in the following definition.

Definition 2 (period-doubling bifurcation). *A smooth, one-parameter family of maps $\{f_a\}$ undergoes a period-doubling bifurcation at a_0 if there exists an open interval I and a positive number ϵ such that*

(1) $a \in (a_0 - \epsilon, a_0 + \epsilon) \Rightarrow \mathrm{Fix}(f_a|_I) = x^*$;
(2) $a \in (a_0 - \epsilon, a_0) \Rightarrow x^*$ *is stable, and* $\mathrm{Per}_2(f_a|_I) = \emptyset$;
(3) $a \in (a_0, a_0 + \epsilon) \Rightarrow x^*$ *is unstable, and* $\mathrm{Per}_2(f_a|_I) = \{x^*_1, x^*_2\}$ *is stable.*

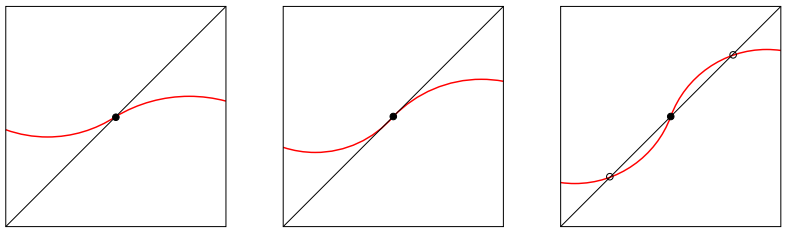

Fig. 8. The period-doubling bifurcation: (a) before, (b) during, and (c) after the bifurcation. Note that we are plotting the second iterate of the map.

Again, we may reverse the direction of the bifurcation with respect to the parameter a. We may also reverse the stabilities, i.e., exchange the roles of stable and unstable in the definition. In the following theorem, explicit conditions are stated that imply the existence of a saddle-node bifurcation. Given a family of maps, the four conditions are easy to check. Again, the proof relies on the implicit function theorem.

Theorem 4 (Period-doubling bifurcation). *Given a C^3 map f, assume that (1) $f_{a_0}(x^*) = x^*$, (2) $f'_{a_0}(x^*) = -1$, (3) $f'''_{a_0}(x^*) \neq 0$, and (4) $\frac{\partial(f_a^2)}{\partial a}|_{a=a_0}(x^*) \neq 0$ hold. Then there exists an interval I containing the fixed point x^*, and a smooth function $p\colon I \to \mathbb{R}$ such that $f_{p(x)}(x) \neq x$, but $f^2_{p(x)} = x$.*

Note that conditions (1)+(2) imply that there is a differentiable curve of fixed points $x^*(a)$ for a near a_0: $f_a(x^*(a)) = x^*(a)$. These conditions also imply that $(f^2_{a_0})''(x_0) = 0$, which means that the graph of f^2 has an inflection point at the bifurcation. Ensuring that the cubic term in the Taylor expansion of f^2 is non-zero (condition (3)) gives rise to the bifurcation illustrated in Fig. 8.

The graph of p describes the location of the period-2 points with respect to the parameter a, see Fig. 9.

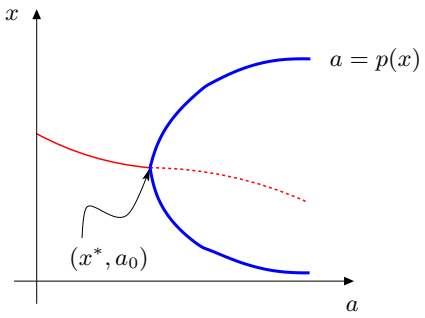

Fig. 9. The period-doubling bifurcation: The thin line represents the fixed point. It is dotted when unstable. The thick line represents the period-2 orbit.

Note that both bifurcations are applicable to the function $g = f^n$, and can thus be carried over to periodic orbits. In the case of the period-doubling bifurcation, this can give rise to a period-doubling *cascade*. This is an infinite sequence of period-doublings, generating the periods $2, 4, 8, 16, \ldots$.

There are many more bifurcations that can occur, especially in higher-dimensional systems. We mention here the *pithfork bifurcation* and the *Hopf bifurcation*, both of which we shall encounter in the final sections.

6 Invariant manifolds

For a C^k vector field $f\colon \mathbb{R}^d \to \mathbb{R}^d$, with a hyperbolic fixed point x^*, we can define its associated *stable* and *unstable* manifolds.

$$W^s(x^*) = \{x\colon \lim_{t\to+\infty} \varphi(x,t) = x^*\}$$
$$W^u(x^*) = \{x\colon \lim_{t\to-\infty} \varphi(x,t) = x^*\}.$$

Analogously, for a C^k map $f\colon \mathbb{R}^d \to \mathbb{R}^d$, we have

$$W^s(x^*) = \{x\colon \lim_{i\to+\infty} f^i(x) = x^*\},$$
$$W^u(x^*) = \{x\colon \lim_{i\to-\infty} f^i(x) = x^*\}.$$

These sets are injectively immersed C^k submanifolds of $\mathbb{R}^d$, and have the same dimensions as their corresponding linear subspaces. If the stable manifold is an open set, then $W^s(x^*)$ is called the *basin of attraction* of x^*. Note that the stable and unstable manifolds are indeed invariant under the dynamical system: as sets they remain unchanged, although individual points are moved about within them. We can extend these definitions to the case when x^* is a periodic point of period n simply by replacing f by f^n.

Knowing the location of a system's fixed points, together with their stable and unstable manifolds gives a very detailed picture of the overall dynamics.

Example 7. Returning to the vector field of Example 2, we illustrate this fact by plotting the stable (blue) and unstable (red) manifolds of the two saddle points, located at $(-1, 1)$ and $(1, -1)$, see Fig. 10. Note that the interior of the region bounded by the stable manifolds of the two saddles constitutes the two-dimensional stable manifold of the spiral sink at $(-1, -1)$, and thus its basin of attraction. In the same manner, the two-dimensional unstable manifold of the spiral source at $(1, 1)$ is bounded by the unstable manifolds of the two saddles.

In the center of Fig. 10(a), we can clearly see a compact region $S = \mathrm{cl}(W^s(-1,-1) \cap W^u(1,1))$. This set is invariant under the flow: $\varphi(S,t) = S$ for all $t \in \mathbb{R}$. The boundary of S contains the four fixed points of the system, and is an invariant set too.

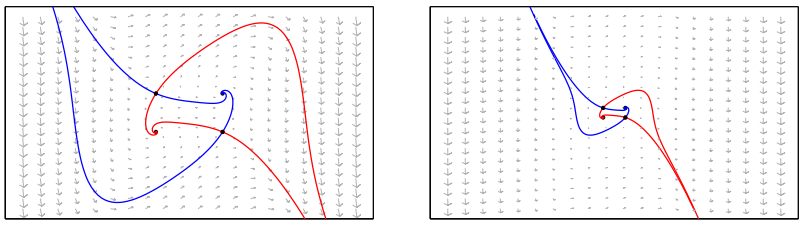

Fig. 10. (a) The stable (blue) and unstable (red) manifolds of the two saddle points. (b) The same invariant sets, but on a larger domain.

Finally, note that points outside $W^s(-1,-1) \cup W^u(1,1)$ are separated into a left part U_L and a right part U_R, see Fig 10(b). Both (invariant) sets lack interesting dynamics: a point is simply transported to infinity both forward and backward in time.

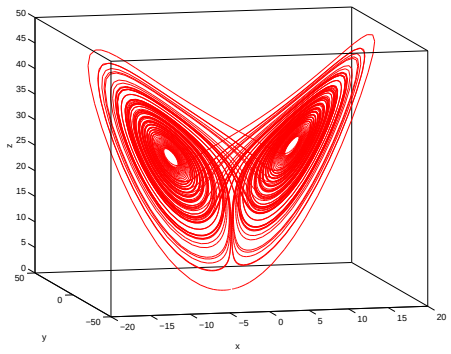

Fig. 11. The one-dimensional unstable manifold of the saddle point.

In general, the stable and unstable manifolds can form very complicated sets. A classic example is the unstable manifold of the origin for the Lorenz equations (more about this system later). In Fig. 11 we show a part of the one-dimensional unstable manifold of the saddle fixed point at the origin.

7 Hyperbolic sets

Let $k \geq 1$, and consider a C^k diffeomorphism $f\colon \mathbb{R}^d \to \mathbb{R}^d$ having a hyperbolic fixed point x^*. According to standard results in spectral theory, there then exists a splitting $\mathbb{R}^d = \mathbb{E}^s_{x^*} \oplus \mathbb{E}^u_{x^*}$, where the invariant subspaces $\mathbb{E}^s_{x^*}$ and $\mathbb{E}^u_{x^*}$ correspond to the spectrum inside and outside the unit circle, respectively.

This means that we can find constants $\sigma \in (0,1)$ and $C > 0$ such that for all $n \in \mathbb{N}$,

$$\|Df^n_{x^*}|\mathbb{E}^s_{x^*}\| \le C\sigma^n \quad \text{and} \quad \|Df^{-n}_{x^*}|\mathbb{E}^u_{x^*}\| \le C\sigma^n$$

for some norm $\|\cdot\|$ on $\mathbb{R}^d$. The subspaces $\mathbb{E}^s_{x^*}$ and $\mathbb{E}^u_{x^*}$ are called the *stable* and *unstable subspaces* for the fixed point x^*. We can extend the notion of a hyperbolic fixed point to a whole set.

Consider a compact set $\Lambda \subset \mathbb{R}^d$ which is invariant under f, i.e., $f(\Lambda) = \Lambda$. We say that Λ is a *hyperbolic set* for f if there exists a splitting $\mathbb{R}^d = \mathbb{E}^s_x \oplus \mathbb{E}^u_x$ for each $x \in \Lambda$, such that

1. $\mathbb{E}^s_x$ and $\mathbb{E}^u_x$ vary continuously with x,
2. the splitting is invariant, i.e., $Df_x \cdot \mathbb{E}^s_x = \mathbb{E}^s_{f(x)}$ and $Df_x \cdot \mathbb{E}^u_x = \mathbb{E}^u_{f(x)}$,
3. there are constants $\sigma \in (0,1)$ and $C > 0$ such that for all $n \in \mathbb{N}$,

$$\|Df^n_x|\mathbb{E}^s_x\| \le C\sigma^n \quad \text{and} \quad \|Df^{-n}_x|\mathbb{E}^u_x\| \le C\sigma^n.$$

7.1 Cone fields

In practice, it is impossible to explicitly find the invariant set Λ, not to mention the splitting $\mathbb{E}^s \oplus \mathbb{E}^u$, except in the most trivial cases. Fortunately, we shall soon see that hyperbolicity is a robust property, and one can thus make do with pretty crude approximations of both Λ and the subbundles of the splitting. By *robust*, we mean that the defining hypotheses are open in the C^1-topology.

Definition 3. *A compact region $N \subset \mathbb{R}^d$ is called a* trapping region *for f provided $f(N) \subset \operatorname{int}(N)$, where $\operatorname{int}(N)$ denotes the interior of N.*

Given a trapping region N, we can construct the *maximal invariant set* of N:

$$\Lambda = \bigcap_{i=0}^{\infty} f^i(N).$$

It is clear that any other invariant set in N must be a proper subset of Λ. Seeing that the sequence $\{f^i(N)\}_{i=0}^{\infty}$ is nested, we can approximate Λ by considering high iterates of N. Any property valid in an open neighborhood of Λ will then also hold for $f^k(N)$ if we take k sufficiently large.

Let $\mathbb{F}^s \oplus \mathbb{F}^u$ be a continuous splitting approximating $\mathbb{E}^s \oplus \mathbb{E}^u$. Given $\alpha \ge 0$ we define the *stable* and *unstable cone fields*

$$C^s_x(\alpha) = \{v_1 + v_2 \in \mathbb{F}^s_x \oplus \mathbb{F}^u_x \colon |v_2| \le \alpha|v_1|\},$$
$$C^u_x(\alpha) = \{v_1 + v_2 \in \mathbb{F}^s_x \oplus \mathbb{F}^u_x \colon |v_2| \ge \alpha|v_1|\}.$$

The following theorem provides a practical way of proving that a set is hyperbolic:

Theorem 5. *Let N be a trapping region for a C^1 diffeomorphism f. Suppose that there exists a continuous splitting $\mathbb{F}^s \oplus \mathbb{F}^u$ defined on N, and that there are constants $\alpha \geq 0$, $C > 0$, and $\sigma > 1$ so that*

$$Df_x^{-1} \cdot C_x^s(\alpha) \subset C_{f^{-1}(x)}^s(\alpha) \quad \text{and} \quad Df_x \cdot C_x^u(\alpha) \subset C_{f(x)}^u(\alpha)$$

and

$$\|Df_x^{-n}|C_x^s(\alpha)\| \geq C\sigma^n \quad \text{and} \quad \|Df_x^n|C_x^u(\alpha)\| \geq C\sigma^n$$

for every $x \in N$. Then $\Lambda = \cap_{i=0}^{\infty} f^i(N)$ is hyperbolic for f.

It is clear that the assumptions of this theorem are open in the C^1-topology, which proves that hyperbolicity is a robust property. In particular, if g is C^1 close to f, then $\Lambda_g = \cap_{i=0}^{\infty} g^i(N)$ is hyperbolic for g.

8 The Smale horseshoe

In this section we will introduce the Smale horseshoe, which was first introduced by Stephen Smale in [Sm67]. The construction is based on a diffeomorphism f defined on a stadium-shaped region N, see Fig. 12(a). It is convenient to think of N as being made up of four pieces: $N = D_l \cup S_l \cup S_r \cup D_r$. Here D_l and D_r are the left and right half discs (coloured blue), respectively. S_l and S_r are the left and right halves of the interior square, respectively. Although the horseshoe map f is well-defined on all of N, all interesting dynamics takes place inside the square $S = S_l \cup S_r$.

The horseshoe map is a composition of a vertical contraction, a horizontal expansion, and a folding. This is illustrated in Fig. 12.

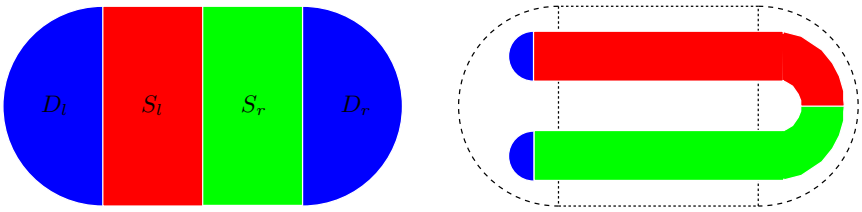

Fig. 12. A geometric description of the horseshoe map.

We will now state some properties of the horseshoe map $f\colon N \to N$.

(1) N is a trapping region for f, i.e., $f(N) \subset N$.
(2) f is injective, but not surjective on N. Thus f^{-1} is not well-defined on all of N.
(3) $f(D_l) \subset D_l$, and f is a contraction on D_l. Thus $f|_{D_l}$ has a unique fixed point p which is a sink: $x \in D_l \Rightarrow \lim_{n\to\infty} f^n(x) = p$.
(4) Since $f(D_r) \subset D_l$, we also have $x \in D_r \Rightarrow \lim_{n\to\infty} f^n(x) = p$.

From (3)+(4) it is clear that the only interesting dynamics (if any) must take place within S: all other points tend to the sink p. We are interested in describing the invariant part of S:

$$\Lambda = \{x \in S\colon f^n(x) \in S \text{ for all } n \in \mathbb{Z}\}. \tag{10}$$

It is natural to think of Λ as the intersection between the set of forward and backward invariant sets: $\Lambda = \Lambda^+ \cap \Lambda^-$, where

$$\Lambda^+ = \{x \in S\colon f^n(x) \in S \text{ for all } n \in \mathbb{Z}^+\}$$
$$\Lambda^- = \{x \in S\colon f^n(x) \in S \text{ for all } n \in \mathbb{Z}^-\}$$

We now assume that f maps the vertical strips V_0 and V_1 linearly onto the horizontal strips H_0 and H_1, see Fig. 13. Let $\Lambda_n^- = \cap_{j=0}^n f^j(S)$. Then we have

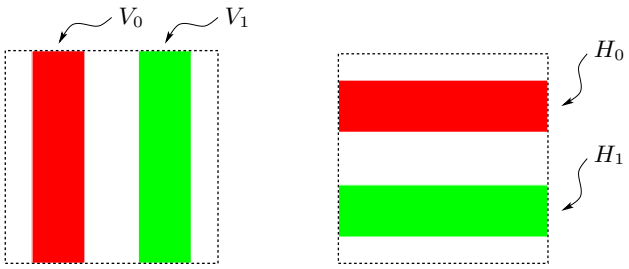

Fig. 13. The horseshoe map acting affinely on the vertical strips V_0 and V_1.

$\Lambda^- = \cap_{j=0}^\infty \Lambda_n^-$, and it follows that

$$\begin{aligned}\Lambda_{n+1}^- &= f(\Lambda_n^-) \cap S = [f(\Lambda_n^-) \cap H_0] \cup [f(\Lambda_n^-) \cap H_1] \\ &= f(\Lambda_n^- \cap V_0) \cup f(\Lambda_n^- \cap V_1).\end{aligned}$$

This means that Λ_{n+1}^- is made up of 2^{n+1} (disjoint) horizontal strips. By the contruction, it follows that the backward invariant set is a Cartesian product of an interval and a Cantor[2] set: $\Lambda^- = I \times C^-$. Analogously, we have $\Lambda^+ = C^+ \times I$, i.e., the forward invariant set is the product of a Cantor set and an interval. Forming the invariant set Λ, we now see that it has a very complicated structure – it is the product of two Cantor sets:

$$\Lambda = \Lambda^+ \cap \Lambda^- = [C^+ \times I] \cap [I \times C^-] = C^+ \times C^-.$$

It can be shown that Λ itself is a Cantor set (of measure zero) on which f displays very complicated dynamics: there is a dense orbit, there are orbits of all periods, and almost all nearby points separate at an exponential rate. It can also be established that Λ is a uniformly hyperbolic set.

[2] A Cantor set is compact, totally disconnected, and consists entirely of boundary points.

8.1 Symbolic dynamics

It is possible to identify the dynamics of the horseshoe map with a synthetic dynamical system: $\sigma\colon \Sigma_2 \to \Sigma_2$. This synthetic system is known as the *full shift on the space of two symbols*, and is defined as follows. Let Σ_2 denote the set of all bi-infinite binary sequences:

$$\Sigma_2 = \{a = (a_i)\colon a_i \in \{0,1\}, i \in \mathbb{Z}\}.$$

In other words, $\Sigma_2 = \{0,1\}^{\mathbb{Z}}$. It is easy to show that Σ_2 is homeomorphic to a Cantor set. We can turn Σ_2 into a metric space by introducing the following notion of distance:

$$d(a,b) = \Sigma_{i=-\infty}^{\infty} \frac{|a_i - b_i|}{20^{|i|}}.$$

We define the *shift map* σ to be the map that takes $a = (a_i)$ to $\sigma(a) = (a_{i+1})$. This is an injective, continuous map, and as claimed above, all dynamical properties of the dynamical system $\sigma\colon \Sigma_2 \to \Sigma_2$ have a counterpart in the horseshoe system $f\colon \Lambda \to \Lambda$. The way this is rigorously established is by proving the existence of a conjugation in terms of a homeomorphism $h\colon \Sigma_2 \to \Lambda$ such that $\sigma = h^{-1} \circ f \circ h$.

The identification between points in Σ_2 and Λ is easy to describe: given a point $p \in \Lambda$, we associate the point $a = (a_i)$ in Σ_2 that satisfies

$$f^i(p) \in V_0 \Rightarrow a_i = 0$$
$$f^i(p) \in V_1 \Rightarrow a_i = 1.$$

The hard part is to establish that h really conjugates the two systems. Taking this for granted, it follows that the following properties of σ carries over to f:

(1) σ has exactly 2^n period-n orbits.
(2) The periodic orbits of σ are dense in Σ_2.
(3) σ has a dense (non-periodic) orbit.
(4) Almost all nearby points in Σ_2 separate at an exponential rate.

A very fundamental observation is that a horseshoe-type dynamics appears whenever a system has a periodic point who's stable and unstable manifolds intersect transversally (also known as a transverse homoclinic point). This was discovered by Poincaré during his work on the stability of the solar system.

9 Attractors

Let $f\colon \mathbb{R}^d \to \mathbb{R}^d$ be a C^k map. We will fix the following notation[3]:

[3] The reader should be aware of that there are several different notions of a strange attractor, see [Mi85]. We choose to use very strong (but natural) requirements in this introduction.

Definition 4. *A compact, invariant set Λ_f is called* attracting *if there exists an open neighborhood U of Λ_f such that $f(U) \subset U$ and $\cap_{i=0}^{\infty} f^i(U) = \Lambda_f$.*

The largest such U is called the basin of attraction for Λ_f, and is denoted $B(\Lambda_f)$. In particular, the maximal invariant set of any trapping region is an attracting set. Even so, it may be the case that most points in $B(\Lambda_f)$ tend to a much smaller subset of Λ_f. As an example, consider a planar diffeomorphism with the phase portrait as illustrated in Fig. 14. Although the whole interval I between the two sinks is attracting with $B(I) = \mathbb{R}^2$, it is clear that most orbits tend to either one of the extreme points of I. Indeed, it is only the points belonging to the stable manifold of the saddle that do not tend to the sinks. In order to rule out this kind of situation, we restrict our attention to

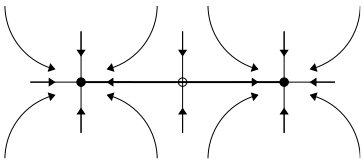

Fig. 14. An attracting set I which is not an attractor.

a subset of the attracting sets.

Definition 5. *An attracting set Λ_f which contains a dense orbit is called an* attractor*: $\Lambda_f = \mathrm{cl}(\cup_{i=0}^{\infty} f^i(x))$ for some $x \in \Lambda_f$.*

This means that Λ_f is minimal in the sense that no proper subset of Λ_f is attracting. Clearly, the attracting set I in our example is not an attractor whereas the two extreme fixed points are. There is, however, nothing "chaotic" about the asymptotic behavior of points tending to these attractors, and the situation is therefore dynamically tame.

From this point of view we would like to be able to distinguish between attractors that exhibit rich dynamics from those that do not.

Definition 6. *An attractor Λ_f is called* strange *if for almost all pairs of different points in $B(\Lambda_f)$, their forward orbits eventually separate by at least a positive constant δ (only depending on Λ_f).*

Here, almost all pairs means with probability one in $B(\Lambda_f) \times B(\Lambda_f)$ with respect to Lebesgue measure. Strange attractors are sometimes called *chaotic* or *sensitive* seeing that, no matter how accurately we measure the initial conditions, we will eventually accumulate an error of size δ.

Sometimes, we can also say something about the speed at which nearby orbits separate. Indeed, if an attractor Λ_f is hyperbolic with a non-trivial unstable tangent bundle, we clearly have exponential divergence of almost all nearby orbits. Such an attractor is called *non-trivial hyperbolic* and, apart from being strange, it is also robust.

All definitions concerning attractors can be carried over to flows by substituting f^i, $i \in \mathbb{N}$ for $\varphi(\cdot, t)$, $t \geq 0$.

10 The Lorenz system

We conclude this short introduction with a presentation of the Lorenz system.

10.1 Global and local bifurcations

The following non-linear system of differential equations, now known as the *Lorenz equations*,

$$\begin{aligned} \dot{x}_1 &= -\sigma x_1 + \sigma x_2 \\ \dot{x}_2 &= \varrho x_1 - x_2 - x_1 x_3 \\ \dot{x}_3 &= -\beta x_3 + x_1 x_2, \end{aligned} \tag{11}$$

was introduced in 1963 by Edward Lorenz, see [Lo63]. As a crude model of atmospheric dynamics, these equations led Lorenz to the discovery of sensitive dependence of initial conditions - an essential factor of unpredictability in many systems. Numerical simulations for an open neighborhood of the classical parameter values $\sigma = 10, \beta = 8/3$ and $\varrho = 28$ suggest that almost all points in phase space tend to a strange attractor - *the Lorenz attractor*.

We first note that the system (11) (and thus its solution) is invariant under the transformation $S(x_1, x_2, x_3) = (-x_1, -x_2, x_3)$. This means that any trajectory that is not itself invariant under S must have a "twin trajectory".

Numerical simulations for parameter values $\sigma \approx 10, \beta \approx 8/3$, and $0 < \varrho < \infty$ indicate that these equations exhibit a strange attractor for an open interval of ϱ-values. This fact was rigorously established in [Tu02]. In what follows, we will see how the solutions change on a global scale as ϱ is varied. This gives us a rough idea of how the chaotic dynamics is created and destroyed.

For $\varrho < 1$, the origin is the only fixed point of the system, and it is a global sink (all three eigenvalues are real and negative).

At $\varrho = 1$, the origin undergoes a pitchfork bifurcation, and for $\varrho > 1$ there are three fixed points: the origin and a symmetric pair of stable fixed points, $C^{\pm} = (\pm\sqrt{\beta(\varrho-1)}, \pm\sqrt{\beta(\varrho-1)}, \varrho-1)$. In the creation of $C^{\pm}$, the origin loses its stability, and becomes a saddle, with one unstable direction. Initially, the symmetric fixed points are sinks, but for ϱ slightly larger than one, two of the negative real eigenvalues become a complex conjugate pair: $C^{\pm}$ have turned into stable spirals. The unstable manifold of the origin, denoted $W^u(0)$, has two branches: one with $x_1 > 0$ ($W^u_+(0)$) and one with $x_1 < 0$ ($W^u_-(0)$. At this stage, $W^u_+(0)$ is attracted to, and spirals toward, C^+, and $W^u_-(0)$ is attracted to, and spirals toward, C^-, see Figure 15.a.

At $\varrho = \varrho_{hom} \approx 13.926$, $W^u_+(0)$ makes such a large spiral around C^+ that it actually hits the stable manifold of the origin, $W^s(0)$. As a consequence, we

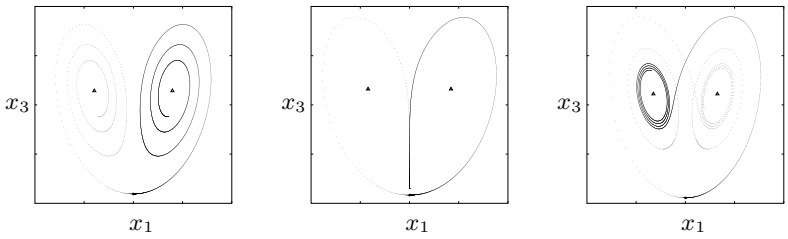

Fig. 15. The Lorenz flow for (a) $\varrho < \varrho_{hom}$, (b) $\varrho = \varrho_{hom}$ and (c) $\varrho > \varrho_{hom}$.

have a homoclinic orbit. By symmetry, we have a pair of homoclinic orbits, see Figure 15.b.

Although it seems intuitively clear, an analytic proof of the existence of these homoclinic orbits was presented as late as 1992 by Hasting and Troy, see [HT92]. They showed that for $\sigma = 10$ and $\beta = 1$, there exists a pair of homoclinic orbits for some $\varrho \in (1, 1000)$.

As mentioned in Section 8, very complicated sets of closed orbits are expected to be created as ϱ is increased beyond ϱ_{hom}. Numerical simulations indicate that the branches of $W^u(0)$ change side before spiraling in towards the fixed points $C^{\pm}$. This results in the creation of two unstable closed orbits and a horseshoe. In 1995, Mischaikow and Mrozek [MM95] showed that for $(\sigma, \beta, \varrho) \approx (45, 10, 54)$, the Lorenz equations do indeed generate a horseshoe, and thus it follows that the Lorenz equations are chaotic for these parameter values. However, the chaotic set (the horseshoe) is not attracting and it has measure zero, whereas the invariant set discovered by Lorenz appeared to be both attracting and large. At $\varrho = \varrho_{het} \approx 24.06$, the branches of $W^u(0)$ enter

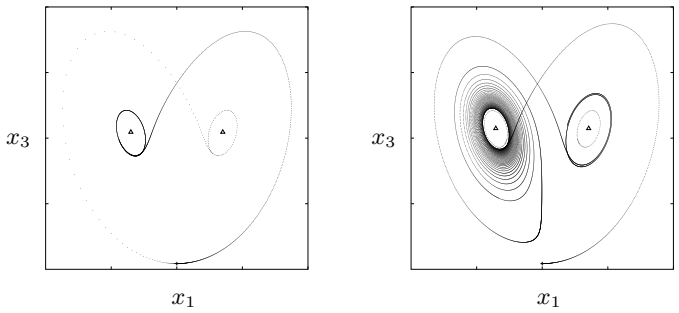

Fig. 16. The Lorenz flow for (a) $\varrho = \varrho_{het}$, (b) $\varrho > \varrho_{het}$.

the stable manifolds of the two unstable closed orbits, see Figure 16.a, thus giving rise to a pair of heteroclinic orbits. This means that both branches wrap around the unstable closed orbits forever. At this stage it seems plausible that the return map may have an attracting invariant set.

For $\varrho > \varrho_{het}$, the branches of $W^u(0)$ spiral outwards from the two unstable closed orbits. When the spirals reach a critical size, they cross over and start to spiral around the other fixed point. This seems to go on for ever.

At $\varrho = \varrho_H \approx 24.74$, the two unstable closed orbits shrink into $C^{\pm}$. The real parts of the complex conjugate eigenvalues of $C^{\pm}$ cross the imaginary axis and become positive as $\varrho > \varrho_H$. This is known as a Hopf bifurcation, and results in $C^{\pm}$ losing their stability, which leaves us with three unstable fixed points.

For ϱ-values greater than roughly 31, there seems to appear intervals where we have stable closed orbits, and for $\varrho \geq 200$ it has been proved in [Ro79] that all solutions tend to a single stable periodic orbit.

We end this introduction with a bifurcation diagram illustrating some of the events described above.

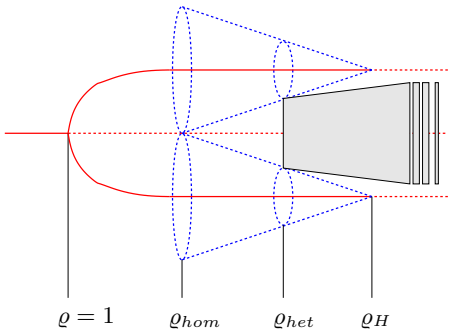

Fig. 17. A bifurcation diagram for $\varrho \in (0, 32)$. Numerical simulations indicate the presence of a strange attractor in the shaded region.

10.2 The dynamics of the Lorenz flow

Recall that for the classical parameter values $\sigma = 10, \beta = 8/3$ and $\varrho = 28$, each fixed point $C^{\pm}$ has a pair of complex eigenvalues with positive real part, and one real, negative eigenvalue. The origin is a saddle point with two negative and one positive eigenvalue satisfying

$$0 < -\lambda_3 < \lambda_1 < -\lambda_2.$$

Thus, the stable manifold of the origin $W^s(0)$ is two-dimensional, and the unstable manifold of the origin $W^u(0)$ is one-dimensional.

We also note that the flow contracts volumes at a significant rate. As the divergence of the vector field is given by

$$\frac{\partial \dot{x}_1}{\partial x_1} + \frac{\partial \dot{x}_2}{\partial x_2} + \frac{\partial \dot{x}_3}{\partial x_3} = -(\sigma + \beta + 1),$$

we see that the volume of a solid at time t can be expressed as

$$V(t) = V(0)e^{-(\sigma+\beta+1)t} \approx V(0)e^{-13.7t},$$

for the classical parameter values. This means that the flow contracts volumes almost by a factor *one million* per time unit, which is quite extreme.

There appears to exist a forward invariant open set U containing the origin but bounded away from $C^{\pm}$. The set U is a torus of genus two, with its holes centered around the two excluded fixed points. If we let φ denote the flow of (11), we can form the maximal invariant set

$$\mathcal{A} = \bigcap_{t \geq 0} \varphi(U, t).$$

Due to the flow being dissipative, the attracting set $\mathcal{A}$ must have zero volume. It must also contain the unstable manifold of the origin $W^u(0)$, which seems to spiral around $C^{\pm}$ in a very complicated, non-periodic fashion, see Figure 11. In particular, $\mathcal{A}$ contains the origin itself, and therefore the flow on $\mathcal{A}$ can not have a hyperbolic structure. The reason is that fixed points of the vector field generate discontinuities for the return maps, and as a consequence, the hyperbolic splitting is not continuous. Apart from this, the attracting set appears to have a strong hyperbolic structure as described below.

As it was very difficult to extract rigorous information about the attracting set $\mathcal{A}$ from the differential equations themselves, a *geometric model* of the Lorenz flow was introduced by John Guckenheimer in the late sixties, see [Gu76]. This model has been extensively studied, and it is well understood today, see e.g. [GW79, Wi79, Sp82, Ra78, Ro89, Ry89]. Meanwhile, the original equations introduced by Lorenz remained a puzzle. During the nineties, however, a few computer-assisted proofs were announced, see [GZ98], [HT92], and [MM95]. These articles deal with subsets of $\mathcal{A}$ which are not attracting, and therefore only concern a set of trajectories having measure zero. Despite this, it was always widely believed that the flow of the Lorenz equations has the same qualitative behavior as its geometric model.

The geometric model is made up of two pieces: one piece dealing with all trajectories passing near the origin, and one piece taking care of the global aspects of the flow. We consider a flow with a fixed point at the origin with eigenvalues just as the Lorenz flow. We also assume that there exists a unit rectangle $\Sigma \subset \{x_3 = 1\}$ which is transversal to the flow, such that the induced return map R acts on Σ as illustrated in Figure 18.

Note that R is not defined on the line $\Gamma = \Sigma \cap W^s(0)$: these points tend to the origin, and never return to Σ. We will assume that $R(\Sigma \setminus \Gamma) \subset \Sigma$, to ensure that the flow has an attracting set with a large basin of attraction. We can now decompose the return map: $R = D \circ P$, where D is a diffeomorphism corresponding to the flow outside a unit cube centered at the origin, and P describes the flow inside the cube. By assuming that the flow is linear in the cube, we can explicitly find P:

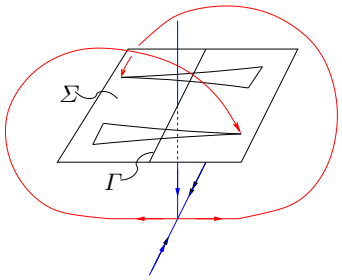

Fig. 18. The two-dimensional return map acting on Σ.

$$P(x_1, x_2, 1) = \big(\operatorname{sign}(x_1), x_2|x_1|^{-\lambda_2/\lambda_1}, |x_1|^{-\lambda_3/\lambda_1}\big).$$

Seeing that $-\lambda_3/\lambda_1 < 1 < -\lambda_2/\lambda_1$, we have very strong expansion in the x_1-direction, and an even stronger contraction in the x_2-direction:

$$\lim_{|x_1|\to 0} \frac{\partial P_3}{\partial x_1} = \mathcal{O}(|x_1|^{|\lambda_3|/\lambda_1 - 1}) \qquad \text{and} \qquad \lim_{|x_1|\to 0} \frac{\partial P_2}{\partial x_2} = \mathcal{O}(|x_1|^{|\lambda_2|/\lambda_1}).$$

The model assumes that the flow outside the cube preserves the x_2-direction, i.e., that D takes the horizontal lines $\ell(t) = (\pm 1, t, c)$ into lines $\tilde{\ell}(t) = (\tilde{c}, t, 1)$, $t \in [-1, 1]$. This ensures that the contracting direction is preserved, and it also implies that the first component of the return map is independent of x_2. Therefore, we can write $R = \big(R_1(x_1), R_2(x_1, x_2)\big)$. Further assumptions are that $\frac{\partial R_2}{\partial x_2} \le \mu < 1$ and $R_1'(x_1) > \sqrt{2}$ for all $x_1, x_2 \in \Sigma$. The return map now has a hyperbolic splitting $\mathbb{E}^s_x \oplus \mathbb{E}^u_x$, with $\mathbb{E}^s_0 = \Gamma$, and the *stable leaves* $\tilde{\ell}(t)$ foliate Σ. Since all points on a stable leaf share a common future, we may form an equivalence class of such points. By taking the quotient, we get an interval map f (note that $f = R_1$), which is assumed to satisfy the following conditions, see Fig. 19:

1. f has a unique singularity at 0 with $f(0^-) = 1$, and $f(0^+) = -1$,
2. $f\colon [-1, 1] \setminus \{0\} \to [-1, 1]$,
3. f is C^1 on $[-1, 1] \setminus \{0\}$, and $f'(x) > \sqrt{2}$ for $x \neq 0$,

These conditions are enough to prove that almost all points in $[-1, 1]$ have dense orbits under f. It is also clear that f exhibits exponential sensitivity. By pulling the information back to the original return map, it is possible to prove that the attracting set of the model flow is a generalized non-trivial hyperbolic attractor (also known as a *singular* hyperbolic attractor).

10.3 The Lorenz attractor

In an issue of *the Mathematical Intelligencer* the Fields medalist Steven Smale presented a list of challenging problems for the 21th century, see [Sm98]. Problem number 14 reads as follows:

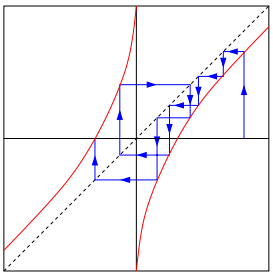

Fig. 19. The one-dimensional return map acting on $[-1, 1]$.

Is the dynamics of the ordinary differential equations of Lorenz that of the geometric Lorenz attractor of Williams, Guckenheimer, and Yorke?

As an affirmative answer to Smale's question, the following result was proved in [Tu02];

Theorem 6. *For the classical parameter values, the Lorenz equations support a robust strange attractor $\mathcal{A}$. Furthermore, the flow admits a unique SRB measure μ_φ with* $\mathrm{supp}(\mu_\varphi) = \mathcal{A}$.

In fact, it is established that the attracting set is a singular hyperbolic attractor: almost all nearby points separate exponentially fast until they end up on opposite sides of the attractor. Loosely speaking, this means that a tiny blob of initial values rapidly smears out over the entire attractor, just as observed in numerical experiments. The existence of the SRB measure is equivalent to saying that, for Lebesgue almost all points in the basin of attraction $B(\mathcal{A})$, and for all $h \in C^0(B(\mathcal{A}), \mathbb{R})$, the time- and space-averages coincide:

$$\lim_{T\to\infty} \frac{1}{T} \int_0^T h(\varphi(x,t))dt = \int h(x)d\mu_\varphi,$$

where μ_φ is an φ-invariant probability measure.

It is perhaps worth pointing out that the Lorenz attractor does not act quite as the geometric model predicts. The latter can be reduced to an interval map which is everywhere expanding. This is not the case for the Lorenz attractor: there are large regions in Λ that are contracted in all directions under the return map. Such regions, however, are pre-compensated by iterates having a large associated expansion. This corresponds to the interval map being eventually expanding, and does not lead to any different qualitative long-time behavior. Apart from this minor discrepancy, the Lorenz attractor is just as the geometric model predicts: it contains the origin, and thus has a very complicated Cantor book structure as described in [Wi79].

References

[Be78] Belitskii, G.R., *Equivalence and Normal Forms of Germs of Smooth Mappings*, Russ. Math. Surv. **33**, 107–177, 1978.

[GZ98] Galias, Z., Zgliczyński, P., *Computer assisted proof of chaos in the Lorenz equations*, Physica D **115**, 165–188, 1998.

[Gu76] Guckenheimer, J., *A strange, strange attractor.* In *The Hopf Bifurcation and its Applications* (Marsden and McCracken, eds.), Springer-Verlag, New York, 1976.

[GW79] J. Guckenheimer, J., Williams, R.F., *Structural Stability of Lorenz Attractors*, Publ. Math. IHES **50**, 307–320, 1979.

[Ha60] Hartman, P., *On local homeomorphisms of Euclidian spaces*, Bol. Soc. Math. Mexicana **5**, 220–241, 1960.

[Ha64] Hartman, P., Ordinary Differential Equations, John Wiley & Sons, New York, 1964.

[HT92] Hasting, S.P., Troy, W.C., *A Shooting Approach to the Lorenz Equations*, Bull. Amer. Math. Soc. **27**, 298–303, 1992.

[HW91] Hubbard, J.H., West, B.H., Differential Equations: A Dynamical Systems Approach. Springer-Verlag, TAM 5, NewYork, 1991.

[Il02] Ilyashenko, Y., *Centennial history of Hilbert's 16th problem*, Bull. AMS **39** No. 3 , 301–354, 2002.

[La82] Lanford, O. E. III., *A Computer-Assisted Proof of the Feigenbaum Conjectures*, Bull. Amer. Math. Soc. 6, 427–434, 1982.

[Lo63] Lorenz, E.N., *Deterministic Non-periodic Flows*, J. Atmos. Sci. **20**, 130–141, 1963.

[MM95] Mischaikow, K., Mrozek, M., *Chaos in the Lorenz Equations: A Computer-Assisted Proof*, Bull. Amer. Math. Soc. **32**, 66–72, 1995.

[Mi85] J. Milnor, On the Concept of Attractor, *Commun. Math. Phys.* **99**, 177–195, 1985.

[Ne64] Nelson, E., Topics in Dynamics I: Flows, Princeton University Press, 1964.

[PT93] J. Palis and F. Takens *Hyperbolicity & sensitive chaotic dynamics at homoclinic bifurcations*, Cambridge University Press, Cambridge, 1993.

[Ra78] Rand, D., *The topological classification of Lorenz attractors*, Math. Proc. Camb. Phil. Soc. **83**, 451–460, 1978.

[Ro79] Robbins, K.A., *Periodic Solutions and Bifurcation Structure at High r in the Lorenz Model*, Siam. J. Appl. Math. **36**, 457–472, 1979.

[Ro95] Robinson, C., Dynamical Systems [2nd edition], CRC Press, New York, 1995.

[Ro89] Robinson, C., *Homoclinic Bifurcation to a Transitive Attractor of Lorenz Type*, Nonlinearity **2**, 495–518, 1989.

[Ry89] Rychlik, M., *Lorenz attractors through a Sil'nikov-type bifurcation. Part 1*, Ergod. Th. & Dynam. Sys. **10**, 793–821, 1989.

[Se85] Sell, G.R., *Smooth Linearization Near a Fixed Point*, Amer. J. Math. **107**, 1035–1091, 1985.

[Si52] Siegel, C.L., *Über die analytische Normalform analytischer Differentialgleichungen in der Nähe einer Gleichgewichtslösung*, Nachr. Akad. Wiss. Göttingen, Math. Phys. Kl., 21–30, 1952.

[Sm67] Smale, S., *Differentiable dynamical systems*, Bull. Amer. Math. Soc. **73**, 747–817, 1967.

[Sm98] Smale, S., *Mathematical problems for the next century*, Math. Intelligencer **20**, No. 2, 7–15, 1998.

[Sp82] Sparrow, C., *The Lorenz Equations: Bifurcations, Chaos, and Strange Attractors*, Springer-Verlag, New York, 1982.

[St57] Sternberg, S., *Local contractions and a theorem of Poincaré*, Amer. J. Math. **79**, 809–824, 1957.

[St58] Sternberg, S., *On the structure of local homeomorphisms of Euclidian n-space – II*, Amer. J. Math. **80**, 623–631, 1958.

[Tu02] Tucker, W., *A rigorous ODE solver and Smale's 14th problem*, Found. Comput. Math. **2:1**, 53–117, 2002.

[Vi97] M. Viana, *Stochastic Dynamics of Deterministic Systems*, Braz. Math. Colloq. **21**, IMPA, Rio de Janeiro, 1997.

[Wi79] Williams, R.F., *The Structure of Lorenz Attractors*, Publ. Math. IHES **50**, 321–347, 1979.